Direct observations on the evolution of shear bands into cracks in metallic glass

Rui-Tao Qu
Shenyang National Laboratory for Materials Science, Institute of Metal Research, Chinese Academy of Sciences, Shenyang 110016, People's Republic of China

Fu-Fa Wu
Shenyang National Laboratory for Materials Science, Institute of Metal Research, Chinese Academy of Sciences, Shenyang 110016, People's Republic of China; and School of Materials and Chemical Engineering, Liaoning University of Technology, Jinzhou 121001, People's Republic China

Zhe-Feng Zhang[a)]
Shenyang National Laboratory for Materials Science, Institute of Metal Research, Chinese Academy of Sciences, Shenyang 110016, People's Republic of China

Jürgen Eckert[b)]
IFW Dresden, Institute for Complex Materials, D-01171 Dresden, Germany

(Received 20 April 2009; accepted 19 July 2009)

The evolution of shear bands (SBs) into cracks was observed by using a high-resolution scanning electron microscope in $Zr_{59}Cu_{20}Al_{10}Ni_8Ti_3$ metallic glassy samples after a small punch test with different strain rates. As shear strain increased along a radial SB, three distinctive regions of morphologies were found (I) bonded SB, (II) microcrack plus bonded SB, and (III) full crack. In region II with moderate shear strain, some glassy "extrusions" were also observed. Once shear offset increases to a critical value, the SB becomes a full crack. For two different SBs in one specimen, the critical shear offsets maintain approximately the same value, which sheds light on the critical shear failure condition of metallic glass. The critical shear offset was also found to be sensitive to the strain rate and a higher strain rate led to less critical shear offset. It is suggested that the structure evolution and heat evolution within a shearing SB should be responsible for the present results.

I. INTRODUCTION

Metallic glass (MG) has been a hot topic during the last decades because of its unique physical and chemical properties. Due to its dislocation-free feature, the strength of MGs approaches the theoretical limit, which gives potential to apply them as structural materials.[1–5] However, the fact that no dislocation exists and thus no slip happens in MG makes it deform and fail mainly by localized shear banding at room temperature.[4,5] Therefore, the evolution of the shear bands (SBs) into cracks should be the key factor controlling the plastic deformation ability of the MGs. While owing to the limited plasticity and the rapid shear failure process,[5] the evolution of SB into crack is hardly observed directly by using the conventional uniaxial tests.

The critical condition for the failure of an SB is also an important issue for the plastic deformation behavior of MGs. In the unconstrained uniaxial tension tests, specimens fail often accompanying with the activity of few SBs and exhibit nearly zero tensile plasticity.[2–5] More recently, large tensile plasticity of ~45% was observed in monolithic MG specimens with submicrometer size,[6] and ~10% tensile plasticity was also reported in bulk MG composites with small dendrites.[7,8] These results intrigued much interest for studying the underlying mechanisms and seeking an effective way to improve the plastic deformation ability of MGs. One innovative concept is the "critical shear offset" proposed by Wu et al.[9–11] for explaining the size-dependent shear fracture of MGs. It is suggested that the specimen will not be broken as long as the shear offset (λ) in any SB is less than a critical shear offset (λ_C), which may only depend on the composition and specific atomic structure. Because the size of sample or dendrites is too small and will refine the major SB shearing to the critical shear offset, the ductility is enhanced.[11] Since the critical shear offset serves as a critical condition for the failure of SBs, it may be helpful not only to show the size-dependent

[a)]Address all correspondence to this author.
e-mail: zhfzhang@imr.ac.cn
[b)]This author was an editor of this journal during the review and decision stage. For the *JMR* policy on review and publication of manuscripts authored by editors, please refer to http://www.mrs.org/jmr_policy
DOI: 10.1557/JMR.2009.0374

tensile plasticity but also to understand the processes of the SBs evolution into cracks. However, due to the ambiguous deformation mechanism of MG, the direct evidence and the physical mechanism of the hypothesis of critical shear offset have not yet been clarified.

Because the small punch test (SPT) can achieve great equivalent plastic strain and profuse SBs,[12,13] even for some brittle MGs like annealed Zr-based MGs that show zero plasticity under compression,[13] it may help researchers to study the shear banding process. During SPT, the plastic deformation of MGs is driven by the steel ball below a puncher subject to compressive loading. The local plastic strain is largest at the center part of an SPT specimen and decreases gradually from center to outside. Therefore, the radial SBs propagate from center to outside and the amount of shear offset in a radial SB varies gradually. When the shear cracking occurs in the center part of a radial SB, the outside part may still be bonded. This provides an effective way to study how the SB evolves into crack. In this work, a high-resolution scanning electron microscope (HRSEM) was used to observe the MG specimens after SPT with different strain rates. By measuring the variation of shear offsets with positions of radial SBs, the processes of shear band evolution were observed and the hypothesis of critical shear offset was also verified. The effect of strain rate on the critical shear offset was discussed as well.

II. EXPERIMENTAL

$Zr_{59}Cu_{20}Al_{10}Ni_8Ti_3$ bulk MG was fabricated by the copper mold casting method. The final ingots were rods with dimensions of $\Phi 3 \times 60$ mm^2. The microstructure was characterized by a Rigaku x-ray diffractometer (XRD; Tokyo, Japan) with Cu K_α radiation. XRD patterns showed that the as-cast alloy had a fully glassy structure. SPT specimens were cut from the MG rods by using an electric spark cutting machine and were then ground and polished into a final thickness of ~95 μm. SPT was conducted in an Instron E1000 mechanical testing machine (Norwood, MA). The two studied specimens were labeled as S1 and S2 and tested with displacement rates of 0.001 and 0.1 mm s^{-1}, respectively. For SPT, the higher displacement rate corresponds to higher local strain rates. After SPT, the specimens were observed under a Leo Supra 35 SEM (Germany) with a resolution of 1 nm to reveal the deformation and fracture features and to quantitatively measure the shear offset.

III. RESULTS AND DISCUSSION

The macroscopic morphologies of two specimens after SPT are shown in Fig. 1. It can be seen that the cracks in sample S1 developed mainly in the center circumferential major SB, and were also observed in several major radial SBs, as shown in Fig. 1(a). Note that for all the radial SBs, the shear offsets decreased gradually from the center part to the outside part. This unique character makes them a good example to study how SB evolves into crack and to directly determine the critical shear offset. Two radial SBs marked as 1st and 2nd SB in Fig. 1(a), due to their good observable clarity, were the objects of this study. The sample S2 at higher local strain rates exhibits a more brittle fracture behavior, as shown in Fig. 1(b). This is consistent with the observation in the previously reported results under compression,[14] in which samples at higher strain rate experienced less compressive plasticity before fracture. The fracture of sample S2 occurred along the radial SBs, similar to the behavior of some brittle MGs reported previously.[10] Because shear deformation decreases along the radial SBs gradually, fracture should also occur gradually from center to outside. This is different from the catastrophic fracture of MGs under uniaxial tests, in which all parts of the major SB fail at the same time.[5]

Figure 2(a) is the whole morphology of the 1st SB in sample S1. One can find that with shear offset increasing, the SB morphology evolves continuously. The whole SB can be divided into three distinctive regions from outside to center with shear strain augmentation. The typical morphologies of these regions were observed at a higher magnification, as shown in Figs. 2(b), 2(c), and 2(d). When shear offset is small (region I), as displayed in Fig. 2(b), all the materials are bonded and no opening cracks can be observed. But in the region near the center part of the sample, which possesses the largest shear strain (region III), as shown in Fig. 2(d), the

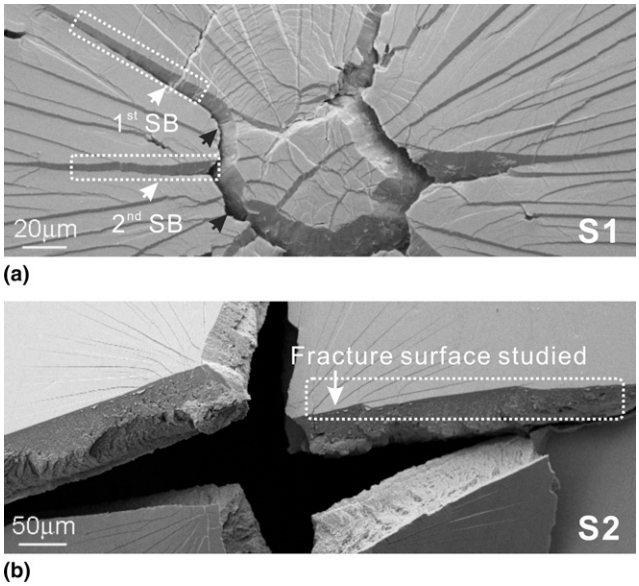

FIG. 1. The macroscopic morphologies of samples after SPT with different displacement rates of (a) 0.001 mm s^{-1} and (b) 0.1 mm s^{-1}. The black arrows in (a) indicate the center circumferential major SB. The white rectangles show the objects studied.

original bonded SB has totally transformed into an opening crack. Additionally, the fracture surface of this shear crack can give some clues of melting phenomenon. Some "veins" were observed on the fracture surface under higher magnification, as marked by the white arrows in Fig. 2(f). Vein pattern is the main feature of the fracture surface of MG specimens subjected to either an unaixal loading test[15,16] or SPT[13] and is often attributed to the fluid meniscus instability of local melting materials.[17,18] In the moderate shear strain region (region II), as shown in Fig. 2(c), it seems to be a mixture state, i.e., both microcracks and still bonded SB can be found. The size of microcracks are ~2 μm and become larger when shear offset increases as the SB approaches to the center. A higher magnification of the bonded area in this region is shown in Fig. 2(e). Interestingly, several glassy "extrusions" were observed, as indicated by the white arrows. It seems that these "extrusions" experienced a low viscosity and were extruded from the SB when SB shearing. The low viscosity implies that the temperature within the shearing SB might be elevated to a certain level in this region.

Similar evolution of SB morphologies with shear offset increment can also been observed in the 2nd SB, as shown in Fig. 3. If we measured the heights of shear steps at different locations of the studied radial SB, the shear offset variation with distance from the center circumferential major SB can be plotted in Fig. 4. For both of the two studied SBs, it is obvious that their shear offsets increased gradually along the radial direction from outside to center, and became approximately the same value of ~4.06 μm. This indicates that the shear offset at this value is just the critical shear offset, i.e., λ_C = 4.06 μm. According to the previous SEM observations, as shear offset increased, the SBs gradually transformed into cracks and presented three distinctive regions, as indicated in Fig. 2(a). In region I, the shear offset (λ < ~2.91 μm) is much smaller than the critical value for crack formation and the SB is totally bonded without any cracks. Furthermore, the shear bands are clean without any hint of temperature rise [see Figs. 2(b) or 3(b)]. With shear offset increasing, i.e., in the region II with a shear offset range of 2.91 to 4.06 μm, some microcracks started to come out and some glassy "extrusions"

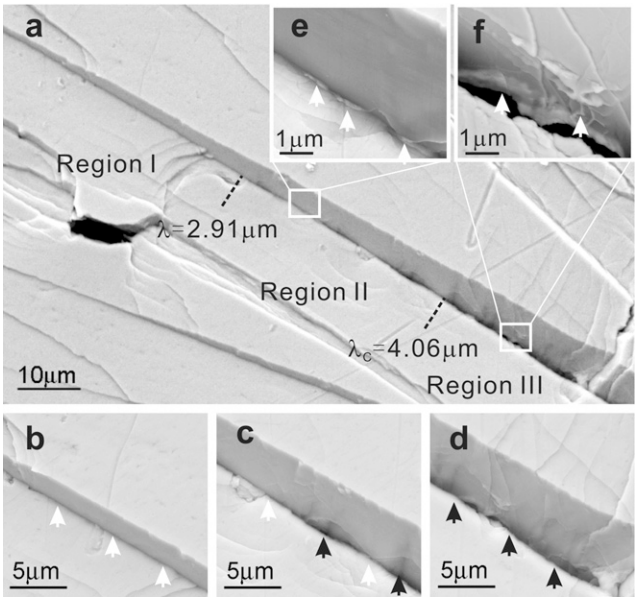

FIG. 2. The evolution of shear band into crack observed in the first SB of sample S1. (a) The whole image; (b)–(d) typical morphologies of three distinctive regions; (e, f) the SEM image at higher magnification. The white arrows in (b)–(d) indicate the bonded SB and black ones point out cracks. The white arrows in (e) show the "extrusions" and those in (f) show the "veins" on the fracture surface.

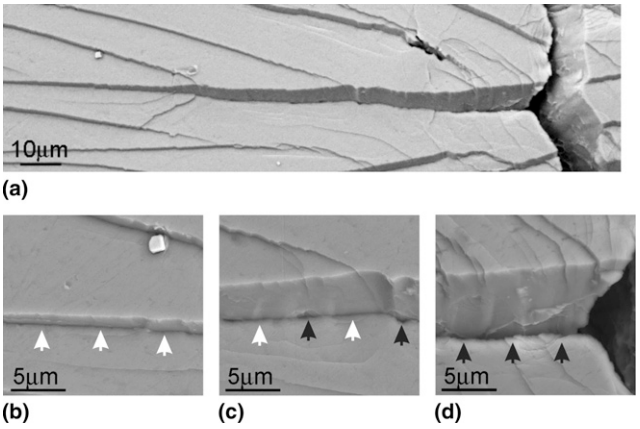

FIG. 3. The evolution of shear band into crack observed in the second SB of sample S1. (a) The whole image; (b)–(d) typical morphologies of three distinctive regions. The white arrows in (b)–(d) indicate the bonded SB and black ones point out cracks.

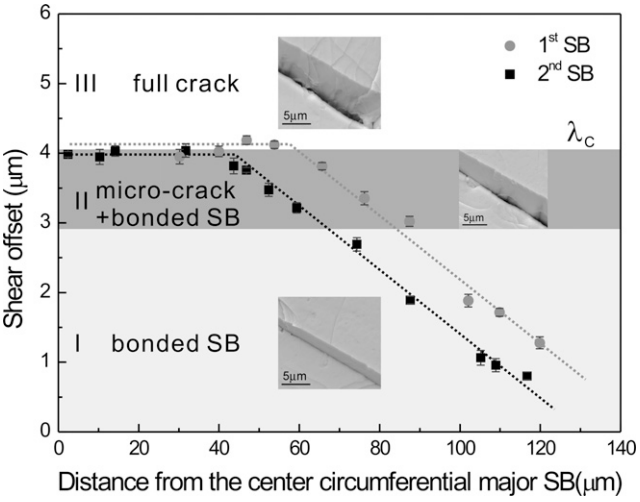

FIG. 4. The shear offset variation of the two studied SBs with the distance from the center circumferential major SB. According to the observations, either the first or second SB presents three distinctive regions: (I) bonded SB, (II) microcracks plus bonded SB, and (III) crack. The boundary between regions II and III is the critical shear offset λ_C.

were observed at high magnification [see Figs. 2(c), 2(e), or 3(c)]. Once the shear offset increased to ~4.06 μm in the region III, the shear band totally became an opening crack and melting phenomenon appeared on the fracture surface [see Fig. 2(f)].

Furthermore, the sizes of smooth regions on the fracture surface of different parts of a gradually fractured radial SB were measured in sample S2, as shown in Fig. 5. We chose 4 areas along the radial direction [see Fig. 5(a)] and observed them in detail. All selected parts of the fracture surface have similar morphologies: smooth region with average size of ~2.41 μm and a dimplelike pattern. The dimplelike morphologies on the fracture surface, similar to those "veins" observed on the fracture surface of a full crack [see Fig. 2(f)], are also closely associated with the viscous flow of MG at fracture accompanying with a dramatic temperature rise.[5,19] Besides, tonguelike materials were observed on the fracture surface near the smooth region, as indicated by the white arrows in Fig. 5. These "tongues" are comparable with the "extrusions" observed in the region II of a radial SB [see Fig. 2(e)]. This further ensures that the "extrusions" along the SB are due to the low glass viscosity. The smooth region is the area that experienced stable shear deformation, thus its size represents the maximum shear amount before fracture.[11] The approximate sizes of smooth regions on the fracture surface indicate that the gradual fracture occurred with the similar shear deformation amount, i.e., the critical shear offset $\lambda_C = 2.41$ μm. This demonstrates that every part of the radial SB will fracture with approximately the same shear amount even though the shear fracture may not happen simultaneously, which further proves the assumption of the critical shear offset as a critical failure condition of SBs.

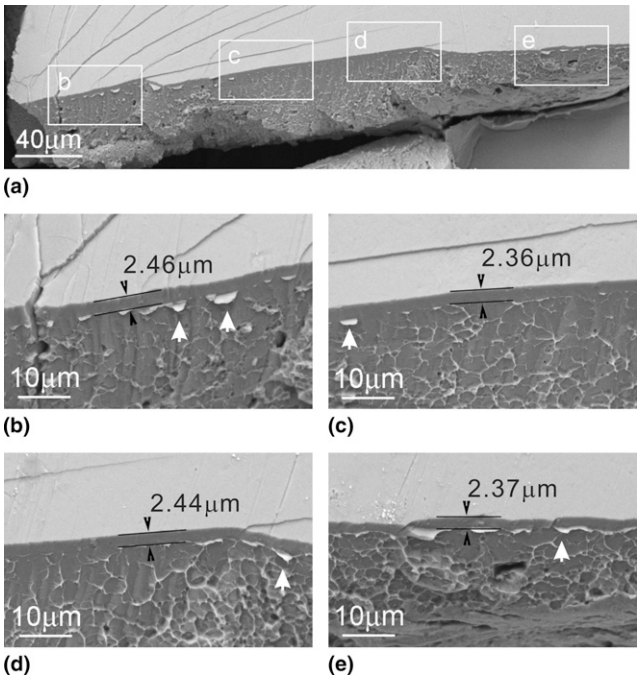

FIG. 5. The fracture surface of sample S2 at a higher displacement rate. (a) The whole fracture surface morphology; (b)–(e) higher magnification images of different areas on the fracture surface. The white arrows show the tonguelike materials.

It should be noted that the critical shear offset λ_C (2.41 μm) of sample S2 that deformed at higher local strain rates is smaller than that (4.06 μm) of sample S1. A similar effect of the strain rate on the size of smooth regions on fracture surfaces was also found in some uniaxial compressive experiments,[14] i.e., a higher strain rate leads to a smaller smooth region size. Although the difference between λ_C under two strain rates is not so large, the results indeed show that the critical shear offset depends not only on the chemical composition and local structure as assumed by Wu et al.,[9–11] but also on the strain rate. To explore the implied reason, based on the previous investigation, it is suggested that the structure evolution and heat evolution within a shearing band should be responsible for the above results.

It has been widely reported that the local structure of an SB changes during shear deformation.[5] As an SB propagates, dilatation is induced and the density decreases,[20–22] and the free volume increases.[23] Nanoscale voids have also been observed in SBs by using transmission electron microscope (TEM).[24–26] Therefore, corresponding to the previously mentioned three regions observed in the gradually deformed SB, we suggest that the whole process of structure evolution within an SB can also be divided into three stages.

A. Stage I: Free volume augmentation and nanoscale void formation

With shear deformation proceeding, the concentration of free volumes in an SB will increase and the dilatation will be induced. By calculating the free energy, it is indicated that these free volumes during shear deformation are unstable.[27] The excess free volumes will coalesce to form voids spontaneously. The size of newly formed voids is always in the order of subnanometers[24] or nanometers[25] and too small to be observed by SEM. Instead, the SB shows only a small shear step on the surface without any cracks, as shown in Figs. 2(b) and 3(b).

B. Stage II: Void growth and microcrack formation

As more shear deformation is gained, the voids will be coarsened and linked.[27] In consequence, some microcracks can be produced at the site of big voids. In the present SPT experiment, some SBs with microcracks were luckily detected by HRSEM, as indicated in Figs. 2(c) and 3(c). Previous researchers using an etching method also showed that microcracks could be formed during plastic deformation,[28] especially in rolling, in which large reduction in

density was found as well.[21] This is consistent with the assumption that the microcracks originate from voids.

C. Stage III: Microcrack development and final fracture

When the size of any microcrack develops to a critical length, with further loading the SB will finally fail and fracture spontaneously. The critical length of microcrack a_c can be estimated by the fracture mechanics,[29] i.e., $a_c = (K_c / Y\sigma_Y)^2 / \pi$, where K_c is the fracture toughness, Y is the geometry correction factor, and σ_Y is the yield strength. In the present SPT specimens, with the shear offset increasing to the critical shear offset λ_C, the radial SBs had totally evolved into open cracks, as shown in Figs. 2(d) and 3(d). Since the critical condition of shear failure described in two different ways, the critical shear offset λ_C should be associated with the critical length of microcrack a_c.

During evolution of SBs, temperature rise inside the SBs should not be neglected. Through an elegant fusible-coating method, Lewandowski and Greer[19] found that there may be thousands of degrees of temperature rise within an SB during its operation. This great amount of heat may remarkably influence the structure and bonding strength of an SB. For instance, with higher temperature rise, the rate of the growth of nanoscale voids may be enhanced[27] and thus more microcracks are easily generated. Hence, the heat evolution inside an SB plays an important role in the failure of the SB. For MG, the heat is generated mainly by the shear deformation.[18] As SB propagation, the thickness of the SB became wider and wider, as observed by TEM.[30,31] The heat-affected zone also behaves in the same way.[31,32] These show that the heat influence can be accumulated as shear deformation developing. Therefore, it is not difficult to understand the observed melting phenomena in region III [see Figs. 2(d) and 3(d)], the glassy "extrusions" in region II [see Fig. 2(e)], and no clear features in region I [see Figs. 2(b) and 3(b)].

The strain rate dependence of the smooth region on the compressive fracture surface was explained by the loss of the ability to accommodate the applied strain rate due to the insufficient rate of SB nucleation.[14] From a heat evolution view, the dynamic loading also makes a small critical shear offset. During shear deformation of MG, besides heat generation, dissipation of heat also takes place. The heat was reported to be generated with a rate of τv, where τ is the applied shear stress and v is the plastic deformation rate.[18] Hence, with higher deformation rate, more heat will be generated in a certain period of time. On the other hand, the heat dissipation is nearly independent on the strain rate but proportional to the elapsed time.[33] Therefore, the higher the strain rate, the more temperature rise within the shear band and the more severe loss of shear resistance. As a result, the critical failure condition of MG at higher strain rate corresponds to a smaller critical shear offset.

IV. SUMMARY

Using an HRSEM, the radial SBs in specimens after SPT, which produced a strain gradient along radial direction, were observed. As shear strain increases, the SB morphology evolves and experiences three distinctive regions. The region I characterize featureless morphology under the smallest shear strain; while microcracks and "extrusions" can be detected only in the region II. When the shear offset increases to a critical value, the SB will transform into a full crack. The studied two SBs in one specimen broke with approximately the same shear offset. Furthermore, the gradually fractured SB has a similar size of smooth region on the fracture surface for different parts of the SB. These results proved the assumption that the critical shear offset is the critical condition for the failure of MG. We suggested that the three regions of morphologies should be associated with the three stages of structure evolution within an SB, including (stage I) free volume augmentation and nanoscale void formation, (stage II) void growth and microcrack formation, and (stage III) microcrack development and final fracture. The glassy "extrusions" in the region II as well as melting materials on the fracture surface suggest that the heat has an accumulative effect. Furthermore, the critical shear offset is found to be dependent on the strain rate, i.e., the higher strain rate, the smaller critical shear offset. This is a result of the greater rate of heat generation at the higher strain rate. Although the critical shear offset may not be an intrinsic parameter, it can be easily measured by SEM and thus can be treated as a convenient and effective critical condition to predict the failure of SBs. What we need to do in the future is to clarify what else influences the critical shear offset.

ACKNOWLEDGMENTS

The authors thank W. Gao, H.H. Su, C.L. Dai, G. Yao, and J.L. Wen for SEM observations and mechanical tests. This work was financially supported by the National Outstanding Young Scientist Foundation under Grant No. 50625103, the National Natural Science Foundation of China (NSFC) under Grant Nos. 50401019, 50871117, and 50890173, and the "Hundred of Talents Project" by Chinese Academy of Sciences.

REFERENCES

1. A.L. Greer: Metallic glasses. *Science* **267,** 1947 (1995).
2. W.L. Johnson: Fundamental aspects of bulk metallic glass formation in multicomponent alloys. *Mater. Sci. Forum* **225–227,** 35 (1996).

3. M.F. Ashby and A.L. Greer: Metallic glasses as structural materials. *Scr. Mater.* **54,** 321 (2006).
4. J. Eckert, J. Das, S. Pauly, and C. Duhamel: Mechanical properties of bulk metallic glasses and composites. *J. Mater. Res.* **22,** 285 (2007).
5. C.A. Schuh, T.C. Hufnagel, and U. Ramamurty: Mechanical behavior of amorphous alloys. *Acta Mater.* **55,** 4067 (2007).
6. H. Guo, P.F. Yan, Y.B. Wang, J. Tan, Z.F. Zhang, M.L. Sui, and E. Ma: Tensile ductility and necking of metallic glass. *Nat. Mater.* **6,** 735 (2007).
7. D.C. Hofmann, J-Y. Suh, A. Wiest, G. Duan, M-L. Lind, M.D. Demetriou, and W.L. Johnson: Designing metallic glass matrix composites with high toughness and tensile ductility. *Nature* **451,** 1085 (2008).
8. D.C. Hofmann, J-Y. Suh, A. Wiest, M-L. Lind, M.D. Demetriou, and W.L. Johnson: Development of tough, low-density titanium-based bulk metallic glass matrix composites with tensile ductility. *Proc. Nat. Acad. Sci. U.S.A.* **105,** 20136 (2008).
9. F.F. Wu, Z.F. Zhang, B.L. Shen, S.X. Mao, and J. Eckert: Size effect on shear fracture and fragmentation of a $Fe_{57.6}Co_{14.4}B_{19.2}Si_{4.8}Nb_4$ bulk metallic glass. *Adv. Eng. Mater.* **10,** 727 (2008).
10. F.F. Wu, Z.F. Zhang, J. Shen, and S.X. Mao: Shear deformation capability of different metallic glasses. *J. Mater. Res.* **23,** 2662 (2008).
11. F.F. Wu, Z.F. Zhang, and S.X. Mao: Size-dependent shear fracture and global tensile plasticity of metallic glasses. *Acta Mater.* **57,** 257 (2009).
12. F.F. Wu, Z.F. Zhang, S.X. Mao, A. Peker, and J. Eckert: Multiplication of shear bands and ductility of metallic glass. *Appl. Phys. Lett.* **90,** 191909 (2007).
13. F.F. Wu, Z.F. Zhang, J. Shen, and S.X. Mao: Shear deformation and plasticity of metallic glass under multiaxial loading. *Acta Mater.* **56,** 894 (2008).
14. T. Mukai, T.G. Nieh, Y. Kawamura, A. Inoue, and K. Higashi: Effect of strain rate on compressive behavior of a $Pd_{40}Ni_{40}P_{20}$ bulk metallic glass. *Intermetallics* **10,** 1071 (2002).
15. Z.F. Zhang, J. Eckert, and L. Schultz: Difference in compressive and tensile fracture mechanisms of $Zr_{59}Cu_{20}Al_{10}Ni_8Ti_3$ bulk metallic glass. *Acta Mater.* **51,** 1167 (2003).
16. Z.F. Zhang, G. He, J. Eckert, and L. Schultz: Fracture mechanisms in bulk metallic glassy materials. *Phys. Rev. Lett.* **91,** 045505 (2003).
17. A.S. Argon and M. Salama: The mechanism of fracture in glassy materials capable of some inelastic deformation. *Mater. Sci. Eng.* **23,** 219 (1976).
18. W.J. Wright, R.B. Schwarz, and W.D. Nix: Localized heating during serrated plastic flow in bulk metallic glasses. *Mater. Sci. Eng., A* **319–321,** 229 (2001).
19. J.J. Lewandowski and A.L. Greer: Temperature rise at shear bands in metallic glasses. *Nat. Mater.* **5,** 15 (2006).
20. D. Deng and B. Lu: Density change of glassy $Pd_{77}Si_{16.5}Cu_{6.5}$ alloy during cold drawing. *Scr. Metall.* **17,** 515 (1983).
21. R.W. Cahn, N.A. Pratten, M.G. Scott, H.R. Sinning, and L. Leonardsson: Studies of relaxation of metallic glasses by dilatometry and density measurements. *Mater. Res. Soc. Symp. Proc.* **28,** 241 (1984).
22. A.S. Argon, J. Megusar, and N.J. Grant: Shear band induced dilations in metallic glasses. *Scr. Metall.* **19,** 591 (1985).
23. A. Vandenbeukel and J. Sietsma: The glass transition as a free volume related kinetic phenomenon. *Acta Metall. Mater.* **38,** 383 (1990).
24. P.E. Donovan and W.M. Stobbs: The structure of shear bands in metallic glasses. *Acta Metall.* **29,** 1419 (1981).
25. J. Li, Z.L. Wang, and T.C. Hufnagel: Characterization of nanometer-scale defects in metallic glasses by quantitative high-resolution transmission electron microscopy. *Phys. Rev. B* **65,** 144201 (2002).
26. W.H. Jiang and M. Atzmon: The effect of compression and tension on shear-band structure and nanocrystallization in amorphous $Al_{90}Fe_5Gd_5$: A high-resolution transmission-electron-microscopy study. *Acta Mater.* **51,** 4095 (2003).
27. W.J. Wright, T.C. Hufnagel, and W.D. Nix: Free volume coalescence and void formation in shear bands in metallic glass. *J. Appl. Phys.* **93,** 1432 (2003).
28. P.E. Donovan and R.F. Cochrane: Deformation-induced microcracking in $Pd_{40}Ni_{40}P_{20}$ metallic glass. *Scr. Metall.* **22,** 1765 (1988).
29. T.L. Anderson: *Fracture Mechanics: Fundamentals and Applications* (CRC Press LLC, Boca Raton, FL, 1995).
30. G. Wang, Y.H. Liu, P. Yu, D.Q. Zhao, M.X. Pan, and W.H. Wang: Structural evolution in TiCu-based bulk metallic glass with large compressive plasticity. *Appl. Phys. Lett.* **89,** 251909 (2006).
31. H. Guo, J. Wen, N.M. Xiao, Z.F. Zhang, and M.L. Sui: The more shearing, the thicker shear band and heat-affected zone in bulk metallic glass. *J. Mater. Res.* **23,** 2133 (2008).
32. Y. Zhang, N.A. Stelmashenko, Z.H. Barber, W.H. Wang, J.J. Lewandowski, and A.L. Greer: Local temperature rises during mechanical testing of metallic glasses. *J. Mater. Res.* **22,** 419 (2007).
33. H.S. Carslaw and J.C. Jaeger: *Conduction of Heat in Solids* (Clarendon Press, Oxford, UK, 1986).